Desalination and Water Treatment
www.deswater.com

doi: 10.1080/19443994.2012.708522

51 (2013) 1494–1502
February

Taylor & Francis
Taylor & Francis Group

Simplified residence time prediction models for constructed wetland water recycling systems

Xiaohua Wei[a,f], Xiugui Wang[b], Bing Dong[b], Xinjian Li[c], Anand K. Plappally[d,e,]*, Zhi Mao[b], Larry C. Brown[a]

[a]*Department of Food, Agricultural and Biological Engineering, The Ohio State University, Columbus, OH 43210-1058, USA*
[b]*State Key Laboratory of Water Resources and Hydropower Engineering Science, Wuhan University, Wuhan 430072, China*
[c]*Guangxi Center Station of Irrigation and Drainage Experiment, Guilin 541100, China*
[d]*Mechanical Engineering Department, Rohsenow Kendall Heat Transfer Lab, MIT, Cambridge, MA 02138, USA Tel. +1 614 5064332; email: plappal@mit.edu*
[e]*Indian Institute of Technology, Jodhpur 342005, Rajasthan, India*
[f]*Maritime Research Centre and School of Civil and Environmental Engineering, Nanyang Technological University, Singapore 639798, Singapore*

Received 27 February 2012; Accepted 28 June 2012

ABSTRACT

The experimental farmland–channel–wetland systems (FCWS) in Guilin, China have been recently designed based on wetland water recycling systems in Midwest USA. The present article develops a methodology for simplifying the prediction of residence time as a function of the flow rate and physical shape of these contaminant removal systems. A series of two-dimensional simulation studies on surface flow through FCWS wetland of different shapes are performed. Parameters influencing hydraulic characteristics such as empirical values of inlet and outlet flow conditions, and wetland shapes are utilized as inputs to the study. Roughness coefficient was assumed to be constant across the different wetland designs discussed in this article. The mean velocity values within the wetland decreases with increase in ratio of variant inlet widths and wetland inflow rates. The results from the simulation are used as inputs for performing a multivariate multiparameter regression algorithm. This framework models the residence time within the wetland independently as a function of shape, mass inflow, and inlet geometry. This simplified model can be used with ease to evaluate existing as well as new wetland system designs for potential improvement in its function of desalting and filtering waters.

Keywords: Constructed wetland; Hydrodynamics; Triangular shapes; Numerical simulation; Multiparameter; Impact factors

1. Background

Land use for wastewater management and treatment is opted following concerns of pollution of fresh waterways and resources. The present paper discusses land application of wastewater in terms of wetlands. The wetlands offer a low-energy intensive elementary water treatment as an alternative [1]. Wastewater is applied to naturally or man-made wetland which act

*Corresponding author.

Presented at the International Conference on Desalination for the Environment, Clean Water and Energy, European Desalination Society, 23–26 April 2012, Barcelona, Spain

as a low-rate filter. Suspended solids are strained out and organic pollutants are absorbed by the soil surface of these wetlands. These water bodies may serve different purposes. First, microbial activities in the wetland soils help to break down organics as well as nutrients. These soils can be very fertile and can be extracted for agricultural uses. Secondly, since the porous soil is saturated with slow moving wastewater for long duration, this process would help in replenishing ground water [2]. Due to their treatment properties, some environmentalists refer wetlands as nature's kidney [3].

The constructed wetlands are constructed for the purpose of wastewater management and treatment system. Wastewater is produced by domestic, industrial, mining, commercial, and agricultural sectors [4]. There are several examples of use of wetland for treatment purposes. For example, constructed wetland treatment is used for purification of water produced during the mining of oil [2,5]. Grismer et al. reported winery effluent treatment using wetlands [6]. Similarly, constructed wetland systems are used in agricultural water treatments too. Farmland–channel–wetland system (FCWS) is an example of this type of system implemented in China [7]. This new system is suitable for agricultural open-channel irrigation systems, and is composed by two parts: farmland and constructed wetlands, which are linked by open channels. FCWS is an adaptation of the wetland reservoir subirrigation system which comprises a wetland and a water reservoir linked to a farm having a subsurface drainage system [8].

The FCWS was introduced in Guilin, China for a rice paddy farmland. The drainage and surface water from the paddy fields are routed to a constructed wetland via a drainage channel, instead of directly to a drainage ditch. The harvested drainage water once treated in the wetland is routed to back to the paddy field through an irrigation channel as shown in Fig. 1.

The wetland connected with the FCWS in Guilin is the plot number 40 as depicted in Fig. 2(a). The dimensions of the plot number 40 are shown in Fig. 2 (b). Agricultural farm runoff flows into the wetland,

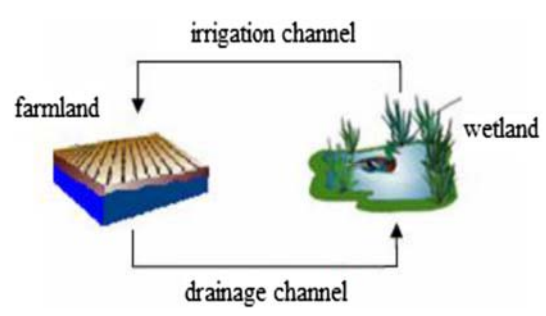

Fig. 1. The FCWS introduced in Guilin [7].

and after treatment the water is reused for irrigating the fields. Wei et al. monitored the variability in constructed wetland flow dynamics as a function of inlet width and inflow rate for this wetland. They also reported that the dynamic pressure and dissipation rates depended on flow inlet geometry of the wetland and the wastewater inflow rate. Wei et al. also demonstrated theoretically that flow rate through this wetland is extremely variable and stochastic [7]. Field observations and flow simulations report short circuiting within plot number 40. Short circuiting is reported to reduce treatment efficiency and alters the normal beneficial biological and chemical transformations which occur within a wetland [10,11]. Nevertheless, little attention has been paid on the analysis of the time that water spends within the wetland and its modeling as a function of wetland shape, inlet geometry, and inflow rate.

Design of constructed wetlands requires general knowledge of hydrology, landscape, soil physics, climate, aquatic biology, civil engineering, ecological engineering, and human requirements of recreation and environment [12,13]. The amount of time that water spends in a wetland will affect the treatment [14,15]. Kroger et al. found that if the time increases, the treatment levels are increased [16]. However, if the flow is turbulent, small particles may not settle even though time in the wetland may be considerable [17]. Another study reported improvement in residence time during summer due to high evapotranspiration [18]. Persson and Wittgren elaborated the design aspects characterizing wetlands. These were vegetation, wetland bottom topography, islands, berms, depth, length–to-breadth ratio, meandering, shape, baffles, and inlet–outlet configurations [19–21]. Numerous studies have performed to investigate the influence of inlet dimensions, shape, vegetation, and flow rate on residence time separately. However, there has been no known model to predict the relationship and enumerate independent influences of each of these variables on residence time.

The purpose of this study is to describe the variation in the flow due to the proposed change in wetland shape. The shapes have been altered keeping the total wetland perimeter in contact with water constant. The shapes were altered to reduce short circuiting and increase recirculation. Inevitable intensive computational flow simulations have been performed and are discussed in the sections below. Although this approach is quite time consuming but provided excellent results. Further, the results gathered from these simulations are incorporated as inputs into a novel stochastic regression modeling framework. This framework will predict residence

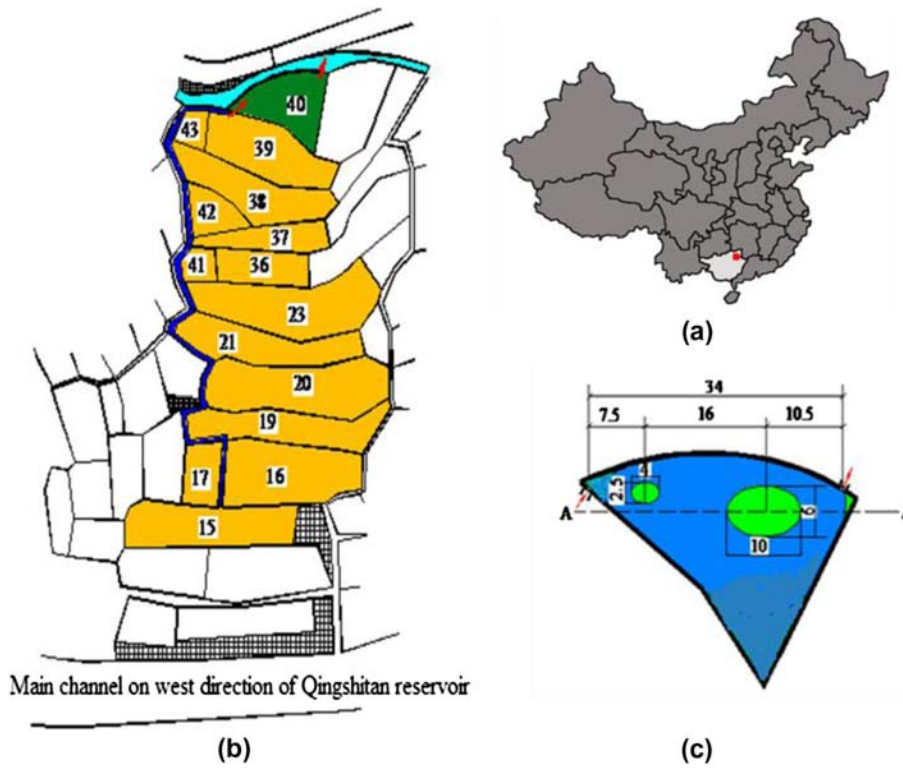

Fig. 2. (a) Depicts Guilin City in Guangxi, China where the FCWS system has been implemented; (b) Illustrates a map showing connected plots of farm lands (colored in yellow) through which water is diverted and finally sent to FCWS wetland in plot No. 40; (c) Depicts the dimensions of the wetland (in meters), the green color in (c) represents islands within the wetland (plot No. 40) [9].

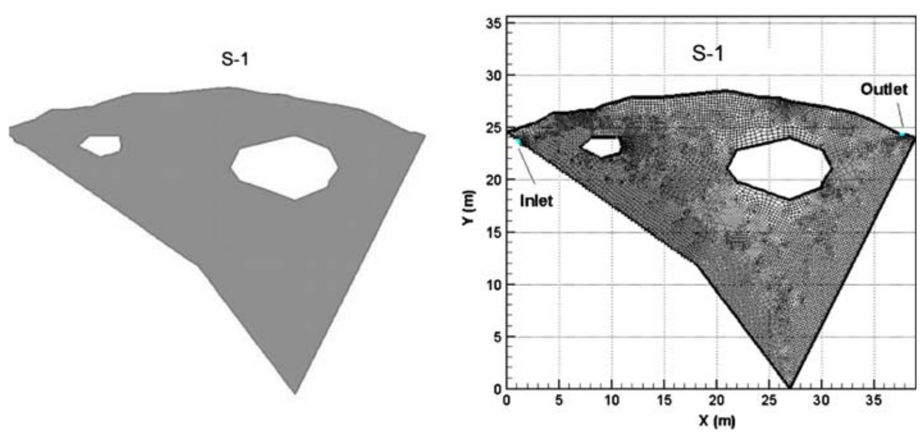

Fig. 3. The original figuration and the simulated grid of wetland S1.

time as a function of inlet dimensions, shape, and flow rate, respectively.

1.1. Current wetland design

The experimental wetland under study at Guilin, China is illustrated in Fig. 3. A detailed report on the functioning of the wetland was performed and documented by the authors elsewhere [9]. For convenience, this experimental wetland is represented in this article with symbol S1. Plants or reed beds within the wetlands help to treat and filter agricultural wastewater. A resistance to flow is also provided by these plants. This resistance is expressed in terms of roughness coefficients. Roughness coefficients imposed in the wetland wall by different plant species were studied by Chow [22]. For the present study, a specific roughness coefficient value of 0.30 was assumed. The wetland S1 has an inlet dimension of 0.5 m. The mesh in Fig. 3 enumerates the dimensions and geometrical features of the wetland.

For in-depth study, the influences of variable inlet width and inflow rate were analyzed and documented in an earlier study [9]. The authors studied flow characteristics of the wetland S1 in Guilin is 2, 20, and 200 kg/s, respectively. A total of 36 cases were studied and simulated flow conditions of drought to flood conditions.

Wei et al. reported variation of velocity within the Guilin wetland (Wetland S1) [7]. Fig. 4 illustrates the velocity profiles of flow within the wetland with inflow rates of 2 kg/s and 200 kg/s, respectively. This flow analysis was performed with varying inlet widths and is enumerated in Fig. 5.

Considering the flow fields in Wetlands S1, maximum velocities exist at the inflow and outflow regions. When inflow rate increases to 200 kg/s (flood condition), the high flow velocities exist at the wetland banks and island boundaries [9]. The mean flow velocities at the triangular zone within the wetland are negligible. Existing maximum velocities within the

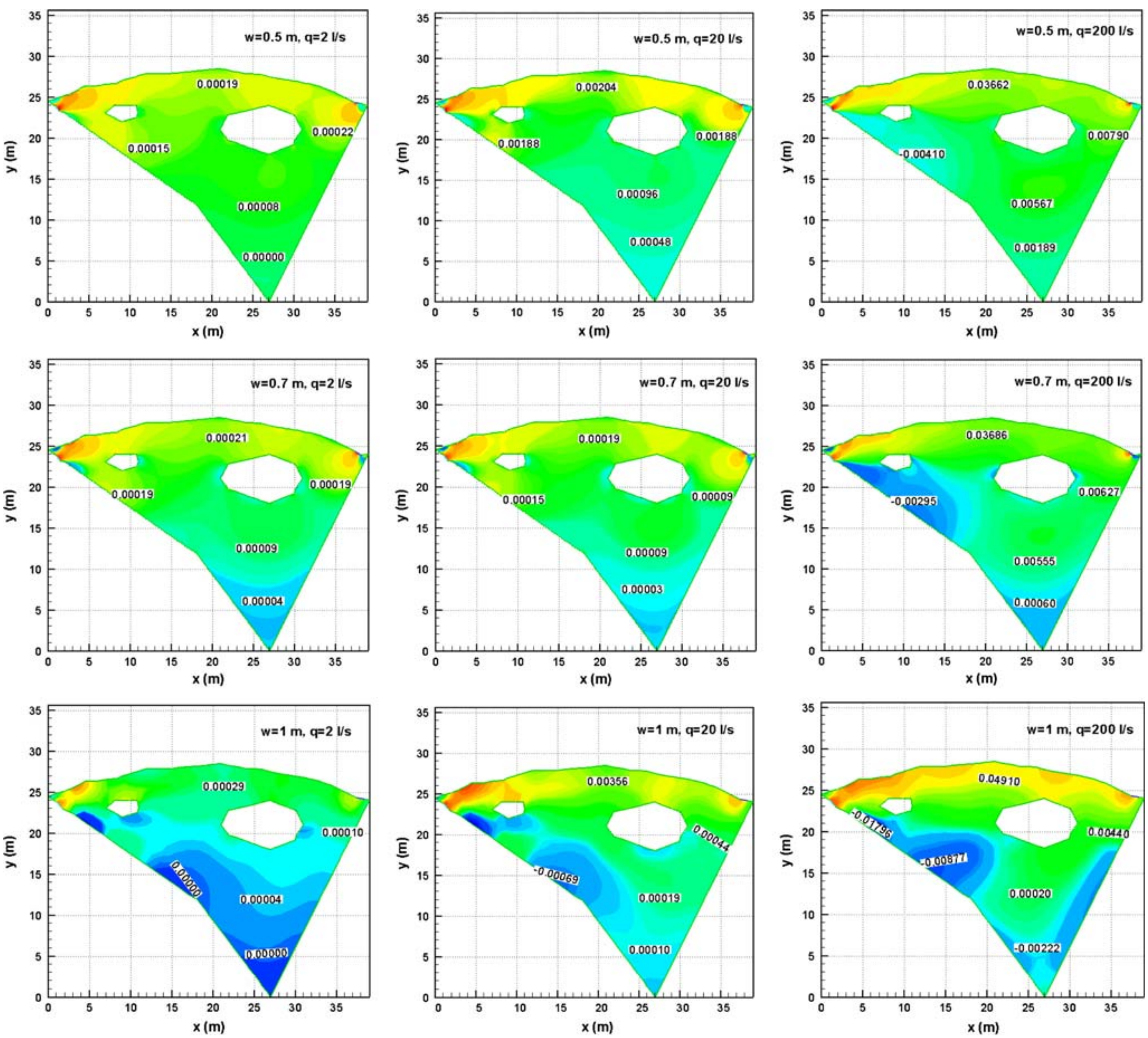

Fig. 4. Comparison of velocity contours with change in inlet width (0.5, 0.7, and 1.0 m) and inflow rate (2, 20, and 200 l/s) of wetland S1.

wetland are directly proportional to the inlet width of the wetland. With increase in inlet width, there is a dip in inflow velocity. Fig. 5 plots a linear curve between normalized velocities in the wetland S1 and normalized inlet width. Wei et al. also found that short circuiting was a prominent feature of Guilin wetland, which did not change with variance in inlet width [7]. The short circuiting is deleterious in the functioning as well as structure of the wetlands [23].

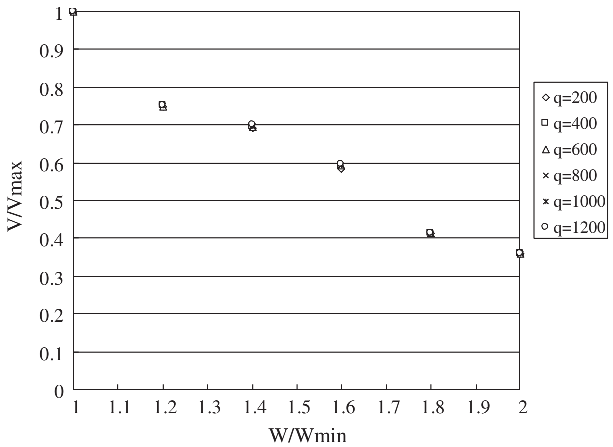

Fig. 5. Relationship among the maximum flow rate, inlet width, and inflow rate of wetland S1.

The major drawback of wetland S1 is short circuiting of flow. This may impair the wetland of its treatment characteristics such as residence time. Short circuiting also decreases the energy dissipating characteristics of wetlands. In order to stop short circuiting and improve the dissipation characteristics of wetlands, a shape change of the wetland is proposed. For present study, shape is varied to maximize residence time as well as to increase the re-circulation zones in the wetlands. This article proposes meandering or zigzag pathways for the wetland in Guilin, China.

1.2. Constructed wetland proposed designs

The new transformations are figuratively represented in Fig. 6. Newly transformed wetland is different from S1. The two construction islands within S1 are removed and a semiellipsoid of the same surface area is introduced at the circular boundary. This newly transformed wetland is named S2. Similarly, another wetland shape was simulated removing the constructed islands and introducing a zigzag-shaped

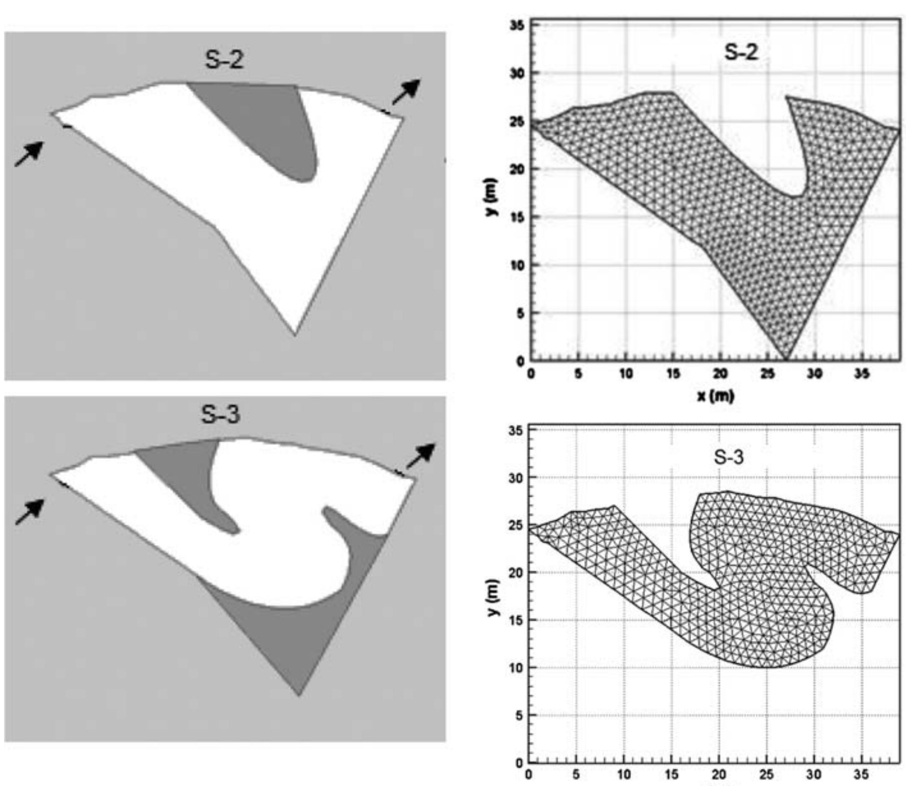

Fig. 6. Transformed wetland designs S2 and S3 based on the original shape of wetland in Guilin, China.

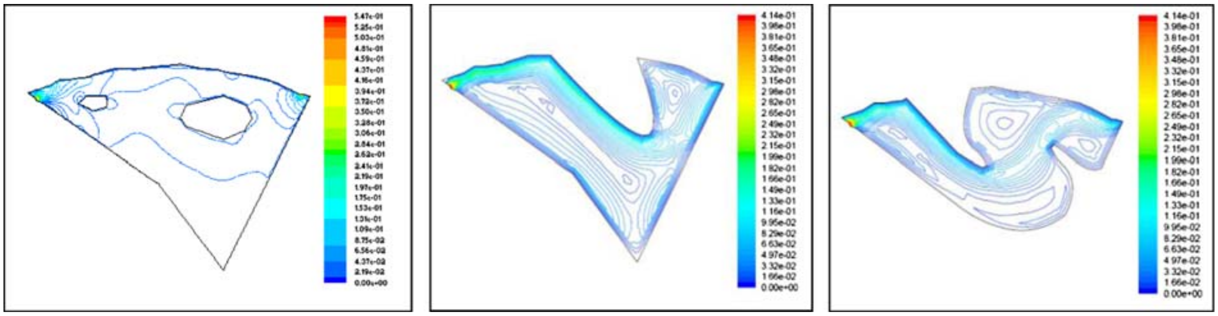

Fig. 7. Velocity magnitude contours.

pattern of the same surface area as the wetland S1, which is named S3. These two new transformations are shown in Fig. 6.

1.3. Methodology introduction

In order to study the flow dynamics within the two wetlands, knowledge of the geometry is required. Fig. 6 also illustrates the dimensions and shape of the newly transformed wetlands. This figure also enumerates the use of a tetragonal grid mesh to project the two-dimensional flow cases under study. Wetlands S1, S2, and S3 are simulated and analyzed. The inlet width (0.5 m) of the wetland was not changed for the new transformations S2 and S3. Inflow rates from 2 to 200 kg/s was assumed. A roughness coefficient of 0.03 was imposed for the flow studies on the three different shapes wetlands.

The flow dynamics within the wetland basin are simulated using Conservation of Mass and Reynolds-averaged Navier–Stokes equations (RANS). The $k \sim \omega$ model is used to simulate flow [24]. This model is a two-equation, eddy-viscosity model, which is used as a low-Reynolds number turbulence model without any extra damping functions. The $k \sim \omega$ model integrates the viscous sublayer flow, and performs well in cases with adverse pressure gradients [25]. Governing equations were solved using Fluent^{TM} [26].

2. Two-dimensional simulated results and analysis

Flow velocity contours for wetlands S1, S2, and S3 are plotted in Fig. 7. It is visible from Fig. 7 that short circuiting in S2 and S3 has reduced and traveling path of the water packets is long compared to wetland S1. The maximum velocity values of wetlands S2 and S3 are equal to 0.414 m/s, while 0.547 m/s for wetland S1; the maximum velocity in these wetlands only happened at inlet. The Fig. 7 also enumerates that peak flow velocities within S2 and S3 are lower than in wetland S1.

Table 1
Inverse flow area in the Guilin wetland S1 and its new transformations of wetland S2 and S3

Different wetland constructions	Percent inverse flow volume
S1	20.9
S2	39.3
S3	43.1

Table 1 tabulates the area of the inverse (recirculation) flow zones for the wetland and its new transformations S2 and S3. Excessive recirculation within the wetland will be beneficial to the objective of elongating the stay of particles within the wetland. A typical estimate of the percent recirculation volumes compared to the total volume within the wetland with an area of 400 m^2 is presented in Table 1. The estimate was completed by plotting the streamlines on a fine graph paper and counting the number of small squares encircled by the recirculation bubbles. From these results, it is noticed that while the recirculation volume is a maximum for S3, it is more than that for S2 and experimental Guilin wetland.

3. Multiparameter analysis

3.1. Nonlinear theoretical development

A nonlinear behavior of average velocity and residence time (Y) is assumed with variation in inflow rate and width of the inlet. A lognormal stochastic multiparameter model has been proposed in this research to model the average velocity, Y, in the wetlands.

The parameters $X_1, X_2, \ldots, X_k$ are manifestations of flow properties as well as geometrical variations. Therefore, Y can be expressed mathematically as follows:

$$Y_i/Y_{i-1} = X_i^{b_i} \quad \text{for } i = 1, 2, 3, \ldots, k \tag{1}$$

where b_i is a constant coefficient for each superposing predictors X_i, for $i = 1, 2, \ldots, k$. With step-by-step injection of k multiple predictor variables, the Y value at $i = k$ can be written as,

$$Y = Y_n = Y_{n-1} X_n^{b_n} = a X_1^{b_1} X_2^{b_2} \ldots X_n^{n} = a \prod_{i=1}^{n=k} X_i^{b_i} \quad \text{for } n = 1, 2, \ldots, k \tag{2}$$

Since the predictor random variables have different dimensions, Eq. (2) can be mathematically reformulated as

$$Y = Y_0 \prod_{i-1}^{k} (X_i/X_{i0})^{b_i} \tag{3}$$

$$a = Y_0 \left\{ \prod_{i-1}^{k} X_i^{b_i} \right\}^{-1} \tag{4}$$

where X_{i0} is any reference constant with the same units as X_i [27].

The initial value of Y_0 is represented by an alphabet "a" for simplicity in Eq. (4). Eq. (2) can be linearized and expressed in the form:

$$y = y_i = \ln Y = \ln a + \sum_{i=1}^{k} b_i \ln X_i \tag{5}$$

3.2. Velocity as a function of the ratio of wetland inlet width to Inflow rate

Additional simulations were performed on the wetland and its transformations S2 and S3 under the conditions of different shapes (S1, S2, and S3), inlet widths (0.5–1.0 m), and inflow rates (200–1200 kg/s). Fig. 8 shows the average wetland velocity plotted against a ratio of variant inlet widths and wetland inflow rates. The average velocity values within the wetland decreases with increase in the ratio of variant inlet widths and wetland inflow rates. At any specific ratio of inlet width to the inflow rate, the average velocity values vary:

$$\overline{v}_{S1} > \overline{v}_{S2} > \overline{v}_{S3}$$

Fig. 8 also depicts a multiplicative relationship between the average velocity, inlet width w, and inflow rate Q as derived theoretically in the earlier section. The nonlinear relationships between average velocity and inlet width/inflow rate are having a high coefficient of determination as illustrated by the R^2 values.

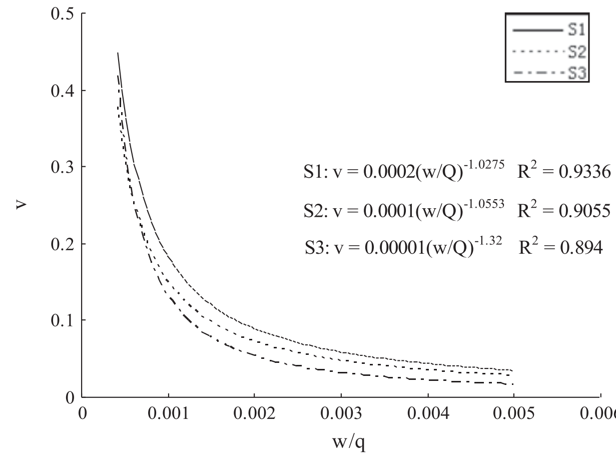

Fig. 8. Relationship among average velocity, inlet width, and inflow rate.

3.3. Time as a function of wetland inlet width and Inflow rate

Fluid packets travel from inlet to outlet. This transport time is dependent on several factors and is a random variable. In this article, this transport time is predicted with random variables of the inlet width "w" and inflow rate "Q". For the convenience of the notation used, w is referred with X_1 while Q is referred with X_2. This prediction equation can be expressed in the form of Eq. (2) and Eq. (5). The summary of coefficients of this prediction of the average time of transport and the improvement in prediction is illustrated in Table 2.

3.4. Travel time as a function of wetland inlet width Inflow rate and wetland shape

In order to include the wetland shape into the model, we introduce a third variable X_3 and define it the shape impact factor. Following the multiplicative relationships found in Fig. 8 and Table 2, the new prediction model including the shape impact factor will be expressed as:

$$y = f(x_1, x_2, x_3) \tag{6}$$

And

$$x_3 = \overline{a} = \ln a \tag{7}$$

Table 2
Summary of model constants prediction transport time in wetlands S1, S2, and S3

Wetland	Independent variables	$\bar{a}$	$\bar{b}_1$	$\overline{b_2}$	R^2	S
S1	X_1	3.79	1.08	0	0.149	0.624
	X_2	3.28	1.08	−1.00	0.998	0.034
S2	X_1	3.83	1.17	0	0.171	0.625
	X_2	3.32	1.17	−1.00	0.998	0.028
S3	X_1	3.81	1.06	0	0.146	0.623
	X_2	3.30	1.06	−1.00	0.998	0.01

Table 3
Model constants of different figuration designs (X_1 is inlet width, X_2 is inflow rate, and X_3 is shape impact factor)

Independent variables	$\bar{a}$	$\bar{b}_1$	$\overline{b_2}$	$\overline{b_3}$	R^2	S
X_1	3.81	1.10	0	0	0.155	0.612
X_2	3.30	1.10	−1.00	0	0.996	0.029
X_3	2.51	1.10	−1.00	0.238	0.998	0.029

The value of variable x_3 is derived from Table 2. This is possible since a is a term which imbibes in itself all the properties of the system is defines [28]. For the validity of linear regression model, all the predictor variables must be independent. The predictor variables X_1, X_2, and X_3 are not correlated to each other, confirming the independence requirement for regression. Table 3 illustrates the summary of the regression carried out and enumerates the improvement in prediction with addition of the predictor variables.

The multiplicative stochastic relationship among wetland design parameters (X_1 is the wetland inlet width, X_2 is the inflow rate, and X_3 is the wetland shape impact factor) and average time Y from inlet to outlet is expressed as:

$$Y = 12.305\ X_1^{1.10} X_2^{-1} X_3^{0.238} \tag{8}$$

Inlet width is found to me the most influencing parameter controlling the variation of residence time of fluid packets within any wetland. Inflow rate applies a negative effect on the average transport time of fluid packets from the inlet to the outlet.

4. Conclusions

Based on the wetland in Guilin, k–ε model in the numerical simulation under different study cases is applied, the flow characteristics in the wetland are analyzed, and also indicated the disadvantage of current wetland design. The improved designs are given subsequently. The wetland flows characteristics under the different designs are compared connecting with multiparameter nonlinear model are evaluated. The conclusions are shown as the following:

(1) The current wetland design should be improved, because of the short circuiting; the improved design should have optimal inverse flow volume to improve residence time.
(2) The impact from the ratio of inlet width to inflow rate on the average velocity of wetland S3 is lowest, while highest of wetland S1;
(3) The average time flowing from inlet to outlet is higher impacted by inlet width than from inflow rate;
(4) The nonlinear relationship among the wetland design parameters (inlet width, inflow rate, and shape) and the average time flow from inlet to outlet is also given in the paper.
(5) A novel stochastic multiparameter regression model for wetland residence time prediction has been developed. It should be noted that vegetation density is assumed to be a constant in this study. The effect of roughness due to presence of vegetation should be studied in future and included to extend the model derived in this article.

References

[1] A. Plappally, J.H. Lienhard, Energy requirements for water production, treatment, end use, reclamation, and discharge, Renew. Sustain. Energy Rev. (in press). http://dx.doi.org/10.1016/j.rser.2012.05.022.

[2] R. Kumar, R.N. Singh, in: T.V. Ramachandra (Ed.), Municipal Water and Waste Water Treatment, TERI, New Delhi, 2006, p. 265.
[3] R.H. Kadlec, R.L. Knight, Treatment Wetlands, Lewis Publishers, Boca Raton, FL, 1996.
[4] K.D. Simeral, Using constructed wetlands for removing contaminants from livestock wastewater, 25 May 1998. http://ohioline.osu.edu/a-fact/005.html (accessed 25.01.11).
[5] M.P.T. Pham, J.W. Castle, J.H.R. Jr, Biogeochemical process approach to the design and construction of a pilot-scale wetland treatment system for an oil field-produced water, Environ. Geosci. 18(3) (2011) 157–168.
[6] M.E. Grismer, M. Tausendschoen, H.L. Shepherd, Hydraulic characteristics of a subsurface flow constructed wetland for winery effluent treatment, Water Environ. Res. 73(4) (2001) 466–477.
[7] X. Wei, A.K. Plappally, A.B.O. Soboyejo, B. Dong, Z. Mao, L. C. Brown, Numerical and multivariate stochastic approaches to characterize flow in a constructed wetland basin, Stochastic Environ. Res. Risk Assess. 26(4) (2012) 545–556.
[8] B.J. Allred, L.C. Brown, N.R. Fausey, R.L. Cooper, W.B. Clevenger, G.L. Prill, G.A.L. Barge, C. Thornton, D.T. Riethman, P.W. Chester, B.J. Czartoski, Water table management to enhance crop yields in a wetland reservoir subirrigation system, Appl. Eng. Agric. 19(4) (2003) 407–421.
[9] X. Wei, L.C. Brown, A.K. Plappally, D. Bin, W. Xiugui, Z. Mao, Hydrodynamics approach to analyzing constructed wetland design, in: Proceedings of the 2nd Cross-Strait Constructed Wetland Conference between the Chinese Mainland and Taiwan, Kaohsiung, Taiwan, 2009, p. 17.
[10] A.F. Lightbody, M.E. Avener, H.M. Nepf, Observations of short-circuiting flow paths within a free-surface wetland in Augusta, Lomnol. Oceanogr. 53(3) (2008) 1040–1053.
[11] J.-H. Min, W.R. Wise, Simulating short-circuiting flow in a constructed wetland: the implications of bathymetry and vegetation effects, Hydrol. Process. 23 (2009) 830–841.
[12] A. Worman, V. Kronnas, Effect of pond shape and vegetation heterogeneity on flow and treatment performance of constructed wetlands, J. Hydrol. 30 (2005) 123–138.
[13] F.E. Dierberg, J.J. Juston, T.A. DeBusk, K. Pietro, B.H. Gu, Relationship between hydraulic efficiency and phosphorus removal in a submerged aquatic vegetation-dominated treatment wetland, Ecological Eng. 25 (2005) 9–23.
[14] J. Koskiaho, Flow velocity retardation and sediment retention in two constructed wetland-ponds, Ecological Eng. 19 (2003) 325–337.
[15] E.L. Thackston, F.D. Shields, Jr., P.R. Schroeder, Residence time distributions of shallow basins, J. Environ. Eng. 113 (1987) 1319–1332.
[16] R. Kroger, M.T. Moore, M.A. Locke, R.F. Cullum, R.W. Steinriede, S. Testa, C.T. Bryant, C.M. Cooper, Evaluating the influence of wetland vegetation on chemical residence time in Mississippi Delta drainage ditches, Agric. Water Manage. 96 (2009) 1175–1179.
[17] WRP, Surface Water Sedimentation Processes in Wetlands, WRP, US-MIL, 1994.
[18] F. Chazarene, G. Merlin, Y. Gonthier, Hydrodynamics of horizontal subsurface flow constructed wetlands, Ecological Eng. 21 (2003) 165–173.
[19] J. Persson, H.B. Wittgren, How hydrological and hydraulic conditions affect performance of treatment wetlands, Ecological Eng. 21(4) (2003) 259–269.
[20] J. Persson, The hydraulic performance of ponds of various layouts, Urban Water. 2 (2000) 243–250.
[21] J. Persson, N.L.G. Somes, T.H.F. Wong, Hydraulics efficiency of constructed wetlands and ponds, Water Sci. Technol. 40 (1999) 291–300.
[22] V.T. Chow, Open Channel Hydraulics, McGraw-Hill, New York, NY, 1959 (Chapter 5).
[23] J.H. Min, W.R. Wise, Simulating short-circuiting flow in a constructed wetland: the implications of bathymetry and vegetation effects, Hydrol. Process. 23 (2009) 830–841.
[24] F. Menter, Two-equation eddy-viscosity turbulence models for engineering applications, AIAA J. 32 (1994) 269–289.
[25] L. Umlauf, H. Burchad, L. Hutter, Extending the $k \sim \omega$ turbulence model towards oceanic application, Ocean Modell. 5 (2003) 195–218.
[26] Fluent 6.3 Manual Fluent Inc (From the Ohio State University), 2006.
[27] A.B.O. Soboyejo, K. Nestor, A new statistical biomechanics approach to modeling of bone strength in broiler chickens and turkeys. Part I-Theoretical development. Part II-Validation of theoretical models, Trans. Am. Soc. Agric. Eng. 43(6) (2000) 1997–2006.
[28] A.B.O. Soboyejo, H.E. Ozkan, J.C. Papritanand, W.O. Soboyejo, A new multiparameter approach to the prediction of wear rates in agricultural sprayer nozzles. Part I—Probabilistic multiparameter model, Part II—Validation of the model, J. Testing Evaluation (JOTE), Am. Soc. Testing Mater. (ASTM), (2001) 373–379.